

# Deep and Statistical Learning in Biomedical Imaging: State of the Art in 3D MRI Brain Tumor Segmentation

K. Ruwani M. Fernando<sup>a,\*</sup>, Chris P. Tsokos<sup>a</sup>

<sup>a</sup>*Department of Mathematics and Statistics, University of South Florida, Tampa, FL, 33620, USA*

---

## Abstract

Clinical diagnostic and treatment decisions rely upon the integration of patient-specific data with clinical reasoning. Cancer presents a unique context that influence treatment decisions, given its diverse forms of disease evolution. Biomedical imaging allows non-invasive assessment of disease based on visual evaluations leading to better clinical outcome prediction and therapeutic planning. Early methods of brain cancer characterization predominantly relied upon statistical modeling of neuroimaging data. Driven by the breakthroughs in computer vision, deep learning became the *de facto* standard in the domain of medical imaging. Integrated statistical and deep learning methods have recently emerged as a new direction in the automation of the medical practice unifying multi-disciplinary knowledge in medicine, statistics, and artificial intelligence. In this study, we critically review major statistical and deep learning models and their applications in brain imaging research with a focus on MRI-based brain tumor segmentation. The results do highlight that model-driven classical statistics and data-driven deep learning is a potent combination for developing automated systems in clinical oncology.

**Keywords:** Brain Tumor, Deep Learning, Medical Imaging, MRI, Segmentation, Statistical Modeling

---

## 1. Introduction

Despite significant progress being made towards understanding the pathophysiology of cancer, its self-sustaining and highly dynamic nature poses several challenges pertaining to cancer detection and treatment monitoring. While technological advancements hold promise in addressing those dilemmas, owing to its complexity, challenges remain in several stages of cancer management, including pre-cancerous lesion detection, tumor segmentation, tumor infiltration, tracing of tumor evolution, prediction of tumor aggressiveness, and recurrence.

Brain Tumors are among the most dangerous malignancies. The unique genetic, epigenetic, and microenvironmental properties of neural tissues confer resistance to treatments (Mackay et al., 2017; Quail and Joyce, 2017), and thus, the clinical management of brain tumors remains a critical challenge. Among tumors arising from the brain, the most predominant are metastases from systemic cancers and gliomas (Bi et al., 2019). Stage IV glioma, referred to as glioblastoma, develops from glial cells and infiltrates the surrounding cell tissues and is the most aggressive form of primary brain tumor, with a median survival of 15 months (Koshy et al., 2012). Brain tumors are often complex in shape and vary greatly in size, texture, and location and thus, the clinical information related to tumors exhibits high spatial and structural variation from patient to patient. Neuroimaging is a pivotal diagnostic tool in disease assessment. While there exists a variety of diagnostic imaging techniques that are in use at present such as X-ray, computed tomography (CT), positron emission tomography (PET), and mammograms, magnetic resonance imaging (MRI) is the method of choice in neurology as

it does not involve the risk of exposure to ionizing radiation. In brain tumor studies, the clinical information embedded in MRI data is vital for analyzing structural brain abnormalities, detecting pre-cancerous lesions, tumor segmentation, and diagnosis.

The segmentation of biomedical images entails delineating pathological regions and is a crucial first step in cancer diagnostic. In the case of glioblastoma multiforme brain tumor (GBM), segmentation involves separating different heterogeneous regions of tumor tissues as the necrotic core, enhancing tumor, and peritumoral edema (swelling in surrounding brain tissues). Different types of imaging modalities provide useful biological information related to tumor-induced neural tissue changes. The T1-weighted (T1), T1-weighted contrast-enhanced (T1ce), T2-weighted (T2), and T2 fluid-attenuated inversion recovery (FLAIR) modalities are the routinely used brain MRI image sequences. A 2D slice of each modality and the segmented scan is depicted in Fig. 1. While segmentation aids in precise localization and diagnosis through objective quantification of tumor tissue composition and size, proper segmentation remains a key challenge due to the intra-tumoral heterogeneity of tumor cells.

Traditional methods of tumor evaluation depend upon qualitative features such as tumor density, intra-tumoral cellular composition, and anatomic relationship to surrounding tissues, which are also termed semantic features. Technological advancements have enabled quantitative assessment of neuropathology facilitating quantification of tumor size, shape, and textual patterns (Aerts et al., 2014; Bi et al., 2019). While early methods of diagnosis relied upon probabilistic tumor models, pivotal breakthroughs in computer vision led to a rapid rise in Artificial Intelligence (AI) research in medical imaging. Deep Learning (LeCun et al., 2015) is a subset of AI that holds great potential to support clinicians in gaining insight from complex, high-dimensional, and heterogeneous biomedical data. Traditionally,

---

\*Corresponding author.

Email address: kfernando@usf.edu (K. Ruwani M. Fernando)

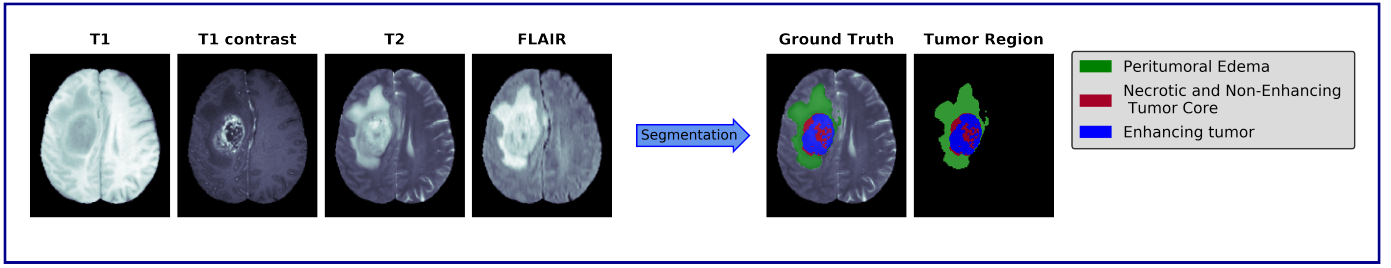


Figure 1: On the left is an example of glioblastoma brain tumor in T1, T1-contrast, T2 and FLAIR modalities. On the right is the ground truth segmentation of the tumor which specifies the class of each voxel.

tional statistics and deep learning vary in their approach for brain tumor quantification, each with its own strengths and weaknesses. Although biomedical image segmentation with statistical modeling and deep learning methods are well-established as independent areas of research, hybridization of the two paradigms is an emerging trend. Going beyond recent retrospective reviews in tumor segmentation which are mostly concentrated on deep learning-based methods, we provide a comprehensive overview linking the two disciplines.

The key contribution of this study towards neuroimaging literature is to provide an integrated overview of statistical modeling and deep learning methodologies for biomedical image segmentation from both a theory-driven and application perspective. Through a comprehensive summary of statistical and deep learning literature, we provide a critical discussion related to the methodologies, limitations, key challenges, and future directions in the area of brain tumor segmentation.

The remainder of this paper is structured as follows: In section 2, we present conceptual bases pertaining to cortical segmentation. Section 3 is a statistical overview comprised of computational theories and recent studies in 3D MRI brain tumor segmentation. This is followed in section 4 by deep learning network architectures in medical imaging and their tumor segmentation applications. Section 5 is comprised of a concise overview of integrated statistical and probabilistic deep learning studies in neuroimaging. Section 6 provides a discussion on limitations, critical challenges, and future directions. Section 7 concludes the paper.

## 2. Brain Tumor Segmentation Preliminaries

Brain imaging analyses rely upon anatomical images of the brain generated by an MRI scanner. The basic concepts in biomedical image segmentation relating to two-dimensional (2D) and three-dimensional (3D) imaging, tumor segmentation process and MRI scan pre-processing are briefly described here.

### 2.1. 2D and 3D Medical Imaging

A 2D image can be defined as a continuous function  $f(s, t)$ , such that  $f: \mathbb{R}^2 \rightarrow \mathbb{R}$ , where  $f(s, t) \in \mathbb{R}$  represents the image intensity level at spatial coordinates  $(s, t) \in \mathbb{R}^2$ . In the case of a 3D image, the function is represented by  $f: \mathbb{R}^3 \rightarrow \mathbb{R}$ , with intensity level  $f(s, t, u) \in \mathbb{R}$  and spatial coordinates  $(s, t, u) \in \mathbb{R}^3$ . An image can be converted into a digital image by sampling the spatial coordinates and quantization of the corresponding intensity

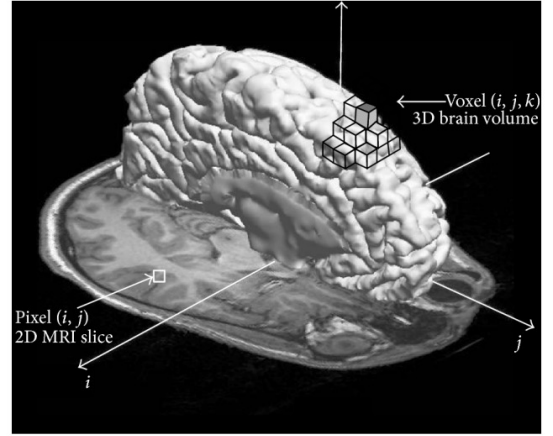


Figure 2: Image elements in the MRI of the brain. An image pixel  $(i, j)$  in 2D space is depicted by the square and an image voxel  $(i, j, k)$  in 3D space is represented by the cube (Despotović et al., 2015).

value. An image that has been discretized in both spatial coordinates and intensity values can be defined on the digital image domain  $D \in \mathbb{Z}^n$ , where  $\mathbb{Z}^n$  represents the  $n$ -dimensional discrete space (Gonzalez and Woods, 2006; Banik et al., 2009). A digital image,  $f(i, j)$  in 2D space and  $f(i, j, k)$  in 3D space, therefore, is composed of a finite number of picture elements uniquely identified by its spatial coordinates and intensity values which are referred to as pixels in 2D space and voxels in 3D space. In a matrix arrangement of pixels,  $i$  denotes the row number and  $j$ , the column number. The MRI scanner generates 3D volumetric brain imaging data as a stack of 2D slices, and  $k$  in the 3D space denotes the slice number. In a standard neuroanatomical volume, isotropic voxel dimension is on the order of 1-2mm. In the 3D space, data is acquired from a series of MRI scans and the resolution of volume data depends upon the in-plane resolution of the 2D cross-sections generated by the MRI scanner. Pixels in 2D space and voxels in 3D space are depicted in Fig. 2 (Despotović et al., 2015).

### 2.2. Tumor Segmentation

Segmentation is the process of partitioning an image into a set of semantically (i.e., anatomically) meaningful and coherent regions, the result of which is either the contours that delineate the region boundaries or the homogeneous region of the structures of interest (e.g., tumors). Let the image domain be denoted by

$\mathcal{I}$  and the segmentation classes by  $k \in K$  where each voxel  $i$  belongs to one of the  $K$  possible classes such that the set  $S_k \subset \mathcal{I}$ . Then the segmentation task involves determining the sets  $S_k$  that satisfies:

$$\mathcal{I} = \bigcup_{k=1}^K S_k \quad (1)$$

where  $S_j \cap S_k = \emptyset$  for  $j \neq k$ .

In the context of medical imaging, segmentation involves identifying the pixels or voxels that represent organs, lesions, and other anatomical substructures. Thus, it enables identifying the extent of an abnormality which can range from the estimation of maximal tumor diameter in 2D measurements to whole tumor assessments and adjacent tissue evaluations in 3D volumetric segmentation. Such information can subsequently be applied in diagnosis, risk assessment, and therapeutic planning.

There are several cortical segmentation clinical applications (Suri et al., 2001) some of which are summarized here. In neurosurgery, *surgical planning* (Schad et al., 1987; Kikinis et al., 1996) is imperative, and segmentation is often the first and the most critical step conducted to identify the 3D coordinates of the tumor cells. Segmentation also aids in *neuro-surgical navigation* (Kosugi et al., 1988; Grimson et al., 1997) to guide the neurosurgeon to move towards the anatomical targets such as tumors while avoiding critical regions of the brain. *Quantitative assessment* (DeCarli et al., 1992) of pathology is vital for establishing treatment strategies and often necessitates segmentation as it allows to quantitatively assess the extent of tumor resection (Cordova et al., 2014) and tumor volume measurements (Wright et al., 1995). By separating image data in anatomical structures into spatially and structurally correlated regions, segmentation enables effective *visualization* (Zeng et al., 1998) of complex biomedical images.

While Segmentation involves separating the image into regions based on homogeneity, classification assigns each voxel to a particular tissue class. For instance, in the case of non-diagnostic neuroimaging classification of brain anatomical structure, tissue classes are gray matter (GM), white matter (WM), and cerebrospinal fluid (CSF). The tasks of segmentation and classification are interconnected on the grounds that segmentation indicates a classification, and a classifier indirectly segments the image. Current clinical practice in oncology is typically dependent upon manually traced segmentation which is time-consuming and subject to inter-observer variability (Warfield et al., 2008) that leads to inconsistent segmentation and poor reproducibility (Hong et al., 2012). Thus, a time-efficient, generalizable, and reproducible automated segmentation process is highly desirable. There are several different segmentation techniques that have been proposed in the past literature, including intensity-based, atlas-based, and surface-based methods, but here we primarily focus on statistical and deep learning voxel-based segmentation.

### 2.3. MRI preprocessing

In structural brain MRI, certain pre-processing steps are required prior to automated segmentation which typically includes image registration, skull stripping, and bias field correction. *Image registration* (Zitova and Flusser, 2003) involves spatially aligning images acquired by different sensors, at different times,

from different viewpoints to a common anatomical space. Inter-patient registration aims at standardizing the images across subjects, whereas intra-patient registration aids in the alignment of imaging modalities (e.g., T1 and T2) within the same subject. *Skull stripping* (Kalavathi and Prasath, 2016) is the process of brain tissue extraction from extra-meningeal tissues such as skull, muscles, or fat and aims at classifying voxels as brain or non-brain. While there are several skull stripping methods available, the most common approach is to use tools such as the brain extraction tool (BET) (Smith, 2002). The intensity inhomogeneity, also known as the *bias field* (Landini et al., 2018; Song et al., 2017) is an undesirable artifact that degrades the segmentation performance leading to quantitative and qualitative misinterpretations. The intensity non-uniformity can be characterized by intensity variation of the same tissue across the MR image. To eliminate the spatial inhomogeneities, several methods have been proposed (Arnold et al., 2001; Belaroussi et al., 2006; Uwano et al., 2014) and N4 bias field correction (Tustison et al., 2010) is one of the widely applied methods at present.

## 3. Statistical model-based 3D MRI Segmentation

Prior art in computational analysis of clinical imaging often relied upon statistical inference. Representative early work in brain tumor segmentation can be categorized into two broad categories: *generative probabilistic models* such as Bayesian-based approaches, Markov random fields and hidden Markov models, and *discriminative models* such as neural networks and conditional random fields (CRFs) (Menze et al., 2014). Generative models incorporate domain-specific prior knowledge related to the anatomy, appearance, and spatial distribution of tissues. For instance, spatial distribution prior for a given set of 3D MRI images can be obtained via lesion-specific biomarkers or by applying a tumor growth model that can be used to deduce the most probable tumor localization. While these methods generalize well to the unseen images, encoding prior information for a tumor is challenging. On the contrary, discriminative models do not incorporate domain knowledge in the learning task but require manually annotated training images. These methods first extract voxel-wise features from the training images such as intensity distributions which are then fed to a classifier for voxel classification and are therefore sensitive to the image intensity profiles. A significant amount of data is required to ensure robustness to imaging artifacts and variations in shape and image intensity.

Three main categories of probabilistic models for cortical segmentation can be identified (Suri et al., 2001): the Bayesian approach, Markov random field (MRF) and expectation-maximization (EM) algorithm. Theoretical aspects of each method and their applications towards brain MRI segmentation are presented here. While the scope of this section is restricted to tumor segmentation, readers can refer to the study by Van Leemput and Puonti (2015) for a more comprehensive overview of brain tissue classification.

### 3.1. The Bayesian Modeling Framework

The Bayesian approach falls under the generative modeling framework and models the probabilistic relationship between segmentation labels and image features such as voxel intensity

values. In the Bayesian framework, the model is fully specified by the prior and the likelihood distribution.

The prior indicates the current state of the knowledge with regard to likely configurations of anatomical structures in the image before the data is observed. Let the segmentation prior distribution be denoted by  $p(\mathbf{y}|\theta_y)$  where  $\mathbf{y} = (y_1, \dots, y_I)^T$  are the labels in an image with  $I$  voxels such that  $y_i \in \{1, \dots, K\}$  represents one of the  $K$  possible anatomical structures assigned to voxel  $i$  and  $\theta_y$  is the set of parameters of prior. Likelihood is the conditional distribution  $p(\mathbf{x}|\mathbf{y}, \theta_x)$  of the voxel intensities  $\mathbf{x} = (x_1, \dots, x_I)^T$  given anatomical labels  $\mathbf{y}$  where  $\theta_x$  is the set of parameters. The segmentation posterior can then be computed via the Bayes' rule with appropriate parameters  $\hat{\theta}$ :

$$p(\mathbf{y}|\mathbf{x}, \hat{\theta}) = \frac{p(\mathbf{x}|\mathbf{y}, \hat{\theta}_x) p(\mathbf{y}|\hat{\theta}_y)}{p(\mathbf{x}|\hat{\theta})} \quad (2)$$

where  $p(\mathbf{x}|\mathbf{y}, \hat{\theta}_x)$  is the likelihood,  $p(\mathbf{y}|\hat{\theta}_y)$  is the prior probability distribution and  $p(\mathbf{x}|\hat{\theta})$  is the marginal distribution with  $p(\mathbf{x}|\hat{\theta}) = p(\mathbf{x}|\mathbf{y}, \hat{\theta}_x) p(\mathbf{y}|\hat{\theta}_y)$ .

Prior and likelihood parametric distributions depend on parameters  $\theta = (\theta_y^T, \theta_x^T)^T$  that are either assumed a priori known or estimated from the image data. The segmentation map of a new image can be estimated via the maximum a posteriori (MAP) estimation which involves maximizing the posterior distribution  $p(\mathbf{y}|\mathbf{x}, \hat{\theta})$  of possible segmentations:

$$\begin{aligned} \hat{\mathbf{y}} &= \arg \max_{\mathbf{y}} p(\mathbf{y}|\mathbf{x}, \hat{\theta}) \\ &= \arg \max_{\mathbf{y}} p(\mathbf{x}|\mathbf{y}, \hat{\theta}_x) p(\mathbf{y}|\hat{\theta}_y) \end{aligned} \quad (3)$$

where  $p(\mathbf{x}|\hat{\theta})$  is a constant that can be excluded.

*Gaussian Mixture Model:* In the segmentation of brain MRI, voxel intensities are typically assumed as independent samples from a mixture of Gaussian distributions. Gaussian mixture model (GMM) presumes that there are similar intensities for voxels in the same tissue class. Based on the assumption that the occurrence of a certain anatomical label in a particular voxel does not depend on the labels in other voxels, the prior distribution is modeled as:

$$p(\mathbf{y}|\theta_y) = \prod_i p(y_i|\theta_y) = \prod_i \pi_{y_i} \quad (4)$$

where parameters  $\theta_y = (\pi_1, \dots, \pi_K)^T$  such that  $\pi_k \geq 0, \forall k$  and  $\sum_k \pi_k = 1$ .  $\pi_k$  denotes the prior probability of a voxel belonging to class  $k$  which is set equal to the relative frequency of each label.

Assuming that the intensity in each voxel is independent of the labels in other voxels and only dependent on the anatomical label in that voxel, the likelihood component of the model has the form:

$$p(\mathbf{x}|\mathbf{y}, \theta_x) = \prod_i p(x_i|y_i, \theta_x) \quad (5)$$

where the product is over all voxels.

Voxel intensity distribution in each tissue class  $k$  can be modeled by a Gaussian distribution characterized by mean  $\mu_k$  and

variance  $\sigma_k^2$ :

$$p(x_i|y_i, \theta_x) = \mathcal{N}(x_i|\mu_{y_i}, \sigma_{y_i}^2) \quad (6)$$

where  $\mathcal{N}(x|\mu, \sigma^2) = \frac{1}{\sqrt{2\pi\sigma^2}} \exp[-\frac{(x-\mu)^2}{2\sigma^2}]$  and  $\theta_x = (\mu_1, \dots, \mu_K, \sigma_1^2, \dots, \sigma_K^2)^T$ .

It can be derived that:

$$p(\mathbf{x}|\theta) = \sum_k \mathcal{N}(x|\mu_k, \sigma_k^2) \pi_k \quad (7)$$

where  $\pi_k, \mu_k$  and  $\sigma_k^2$  are prior, mean and variance of class  $k$ , respectively. Thus, in the GMM, each voxel's intensity distribution is described by a linear superposition of  $K$  Gaussians.

Early studies, as well as current work, investigated the applicability of Bayesian methods for MRI segmentation. For example, in the formative work of Shattuck and Leahy (2002), authors presented a cortical surface identification process from MR images and applied a Bayesian strategy for voxel-based tissue classification. Corso et al. (2008) proposed a Bayesian formulation to calculate affinities in the segmentation of glioblastoma multiforme brain tumor and showed that the incorporation of model-aware affinities improves segmentation results. Pate-naude et al. (2011) modeled the probabilistic relationships between both shape and intensity using a Bayesian approach which exhibited improved performance in structural segmentation of brain images in terms of accuracy and robustness. A GMM based on variational Bayesian inference for brain MRI image segmentation was proposed by Xia et al. (2016). However, their approach requires training a large number of variational models which is computationally expensive. In a recent study by Lipkova et al. (2019), authors integrated structural and metabolic scans and modeled the tumor density of glioblastoma patients using a tumor growth model under the Bayesian framework.

While Bayesian MRI segmentation is a well-studied problem, they necessitate the use of prior information and the analysis is sensitive to the choice of the prior. When encoding prior knowledge robustness of the prior must be ensured so that the conclusions are not affected by the form of the prior distribution. Further, assuming spatial independence between voxel intensities is not justifiable and may lead to voxel misclassifications. The probabilistic tumor model should therefore incorporate context and characterize the true shape of anatomical structures.

### 3.2. Modeling spatial context with Markov Random Field

A voxel intensity value is statistically dependent on the intensity of neighboring voxels. Markov random field (MRF) allows modeling the spatial context by integrating voxel dependencies in the image surface. An MRF can be characterized by a graph  $\mathcal{G} \triangleq (\mathcal{H}, \mathcal{N})$  with  $\mathcal{H}$  representing a lattice containing nodes and  $\mathcal{N}$  indicating the links between the nodes, such that the neighboring relationship of nodes is defined by  $\mathcal{N} = \{\mathcal{N}_i | \forall i \in \mathcal{H}\}$ , where  $\mathcal{N}_i$  is the neighborhood around a position  $i$  (Li, 2009). This graphical structure is comparable to a 3D image grid with nodes representing the voxels and edges, the spatial dependency between voxels. For example, each voxel in a 3D image has 6 direct neighbors.

Assuming that the voxels with the same labels are a part of the same cluster, the MRF model formulates the prior distribution

$p(\mathbf{y}|\theta_y)$  as (Van Leemput and Puonti, 2015):

$$p(\mathbf{y}|\theta_y) = \frac{1}{Z(\theta_y)} \exp(-E(\mathbf{y}|\theta_y)) \quad (8)$$

where  $E(\mathbf{y}|\theta_y)$  is an energy function and  $Z(\theta_y) = \sum_{\mathbf{y}} \exp(-E(\mathbf{y}|\theta_y))$  is a normalizing constant that guarantees  $\sum_{\mathbf{y}} p(\mathbf{y}|\theta_y) = 1$ .

Energy function typically takes the form,

$$E(\mathbf{y}|\theta_y) = \beta \sum_{(i,j)} \delta(y_i \neq y_j) \quad (9)$$

where the summation is over all the neighboring voxel pairs.  $\beta$  is a parameter that regulates the amount of penalization for undesired configurations. If  $k = y$  then  $\delta(k \neq y) = 0$  and 1 otherwise. Thus, the energy function promotes spatially clustered labels.

The MRF model reduces the effect of statistical noise in highly noisy data and the potential number of misclassified voxels and has been successfully applied in many studies. Capelle et al. (2000) presented an unsupervised MRF-based segmentation approach to detect the presence of tumors. Each homogeneous region, healthy and tumor brain tissues, can be considered as a single texture. The texture number in the segmentation field is unknown a priori, which motivates the use of an unsupervised approach. They applied MRF as it classifies each pixel by considering the neighborhood dependency of pixels, where they then estimated realization of the hidden Markov field via a maximum a posteriori estimator (MAP). Gering et al. (2002) proposed a brain tumor segmentation framework where they first trained on healthy brains to diagnose brain tissue abnormalities and then used a multi-layer MRF framework combined with an extended EM-based segmentation. They incorporated contextual information on several layers in the segmentation process which included intensities of voxels, structural coherence, intra and inter-structure properties, and user input. However, this approach has certain limitations as high-level layer classification is sensitive to the noise in the lower layers. Bauer et al. (2011) utilized an MRF-based tumor growth model together with atlas-registration for volumetric MRI brain tumor segmentation. To ensure atlas and patient MRI scan correspondence, the tumor growth model is devised as a mesh-free MRF Energy Minimization problem. Their method is non-parametric and can be applied for tumor mass-effect simulations which facilitate the atlas-based segmentation. More recently, Rajinikanth et al. (2017), applied the MRF-EM combination in conjunction with a firefly-assisted algorithm for 2D MRI tumor segmentation. During the process of segmentation, MRF assigns the label of each pixel to one of the three categories: white matter, gray matter, and tumor mass. Their results suggest that the proposed approach is a better alternative compared with the other methods tested in their study.

While the MRF model allows integrating prior that incorporate spatial context, computing the posterior explicitly is computationally expensive and requires the use of approximation schemes. Thus, MRFs have shortcomings with respect to computational efficiency.

### 3.3. Parameter optimization with Expectation Maximization Algorithm

Obtaining reliable parameter estimates is crucial in statistical model-based segmentation. To estimate appropriate model parameters  $\hat{\theta}$ , the maximum likelihood approach can be adopted which attempts to estimate the setting of the parameter vector  $\theta$  that maximizes  $p(\mathbf{x}|\theta)$ ,

$$\begin{aligned} \hat{\theta} &= \arg \max_{\theta} [p(\mathbf{x}|\theta)] \\ &= \arg \max_{\theta} [\log p(\mathbf{x}|\theta)] \end{aligned} \quad (10)$$

where  $p(\mathbf{x}|\theta)$  represents how likely is an image  $\mathbf{x}$  for a given set of parameters  $\theta$ .

The expectation-maximization (EM) framework allows obtaining maximum likelihood estimates of unknown parameters which is a common strategy in tumor segmentation when modeling MRI intensities of brain tissues as Gaussian mixtures. The parameters in brain tissue segmentation may include intensity, bias correction, and registration parameters. The EM algorithm iterates between two steps until convergence: the *expectation step* (e-step) and the *maximization step* (m-step). In brain tissue segmentation, the model parameter estimates are often initialized via a GMM. Then, in the E-step the model seeks to estimate the tumor segmentation where each pixel/voxel is assigned to a cluster under the current model parameter estimates of the posterior distribution and the M-step estimates the model parameters based on the current classification.

There exists a considerable body of literature on tumor segmentation where the EM algorithm was incorporated in conjunction with the hidden Markov random field (HMRF) Model (Zhang et al., 2001; Nie et al., 2009; Doyle et al., 2013). For example, in the prominent work by Zhang et al. (2001), authors showed that a 3D fully automated brain MR image segmentation which is both accurate and robust can be achieved through an HMRF-EM framework. HMRF framework aids in encoding spatial information of neighboring sites and the model parameters are estimated via maximum likelihood estimation using the EM algorithm. Moon et al. (2002) proposed a model-based approach for segmenting healthy and tumor brain tissues from 3D MRI, where they used a probabilistic geometric model coupled with the EM algorithm. They extended the spatial prior of a probabilistic normal human brain atlas with tumor information obtained from patient data to include spatial prior for tumor tissues. A generalized EM segmenter via a generative probabilistic modeling approach for brain lesion segmentation was introduced by Menze et al. (2015) which demonstrated improved generalization.

The EM algorithm ensures that likelihood increases with each step and frequently used when the model depends on latent variables. Nevertheless, it exhibits slow convergence and may only converge to local optima.

*Summary:* Justifying the underlying probability distribution that drives data is an important facet in statistical model-based methods of segmentation. These methods have the intrinsic limitations of requiring domain expertise and knowledge of prior distribution. Translating information about prior knowledge into a probabilistic model can be challenging and inference may involve extensive computations. These shortcomings restrict their

deployment in large-scale and time-sensitive applications. However, model-based approaches are effective in terms of the model interpretability and the amount of data required for the analysis.

#### 4. Deep Learning based 3D MRI Brain Tumor Imaging

Deep Learning (DL) excels at the extraction of complex feature representations that cannot be perceived by the human brain enabling quantifiable image interpretation. Previous studies have exploited different architectures of deep networks for biomedical image segmentation, varying from unique convolutional neural net based architectures to probabilistic deep generative models. In this section, we present widely adopted deep learning architectures in recent literature and their practical applications in 3D multi-modal MRI brain tumor segmentation.

##### 4.1. Convolutional Neural Networks

Recent years have seen a proliferating use of convolutional neural networks (CNNs) (LeCun et al., 1999) in medical image analysis owing to their ability to integrate structural information contained in adjacent pixels. CNNs are comprised of multiple convolutional and pooling layers stacked sequentially. By convolving a filter (also referred to as kernel) across the input and performing a convolution operation, a convolutional layer generates feature maps, which are then passed through an activation function such as Rectified Linear Unit (ReLU) for non-linear transformation. The output feature map is then fed to a pooling layer for down-sampling. The fully connected layer placed at the end of the network maps the features extracted by convolutional and pooling layers into the final output and make the final prediction.

In contrast to the conventional DL classifiers such as AlexNet (Krizhevsky et al., 2017), VGGNet (Simonyan and Zisserman, 2014) and GoogLeNet (Szegedy et al., 2015), which takes an image as the input and output a probability distribution over all classes with regard to the entire image, the task of segmentation requires a per-pixel classification of the input. This can be achieved by feeding the classifier with patches extracted around each pixel and adopting a sliding-window strategy (Fig. 3). Semantic segmentation in the computer vision domain typically involves 2D images, consequently, the methods developed for segmentation are mainly based on 2D methods. Therefore, deep learning in 3D volumetric medical image segmentation calls for modifications on architectures that are developed for semantic segmentation. While some studies showed promising results when applying 2D CNN architectures to process 3D volumes in a slice-by-slice manner, for example in (Ciresan et al., 2012; Zikic et al., 2014; Pereira et al., 2016; Havaei et al., 2017), it is arguably a sub-optimal use of the 3D clinical image data as it is time-inefficient and fails to leverage contextual information from adjacent slices.

*3D Convolutional Neural Networks:* 3D CNNs, as a generic extension of 2D CNNs capable of extracting volumetric representations with the use of 3D kernels have received significant attention in neuroimaging. In the seminal work of Kamnitsas et al. (2017c), a 3D CNN based architecture, termed *DeepMedic*, was introduced for automated brain lesion segmentation of 3D volumetric brain scans and ranked at the top in the Ischemic Stroke Lesion Segmentation (ISLES 2015) challenge. They

conducted a patch-based analysis using a dual pathway strategy which allows feeding the network a version of the image at multiple scales concurrently, facilitating the incorporation of both local and global contextual information. This process was further improved later with several architectural modifications (Kamnitsas et al., 2017a).

While patch-wise segmentation with CNNs does not require major architectural adaptations, it is computationally expensive and entails redundant operations since adjacent pixels in an image are similar in the vicinity of the pixel being processed and the input patches from adjacent pixels are overlapped. In addition, the smaller the patch size, the network has less possibility of learning the global context as the learning process is confined to visible features in each patch.

##### 4.2. Multi-stream architectures

The integration of contextual 3D information can also be performed through multi-stream architectures. While the standard CNN can incorporate multiple sources of information through the channels in the input layer, multi-stream architectures enable merging the channels at intermediate points in the network. They enable fusing features extracted from multi-angled patches from the 3D space (three patches from the orthogonal views of an MRI volume), an approach known as 2.5D method (Roth et al., 2014), which incorporates (partial) 3D information from neighboring slices using 2D kernels that results in lower computational cost, but less powerful volumetric representations than in 3D CNN. The multi-path approach also facilitates combining patches of different scales (2D, 2.5D, 3D patches), where each branch contains a CNN corresponding to each patch type. Farabet et al. (2012) introduced multi-stream multi-scale architecture in natural images, and later the idea was implemented by several authors in the context of medical imaging (Roth et al., 2015; Setio et al., 2016; Kamnitsas et al., 2017c; Moeskops et al., 2016). However, multi-stage training schemes can be susceptible to overfitting.

Despite the increased use of 3D CNNs and their 2D/3D hybrid variants, these methods are associated with limitations such as computational complexities due to increased number of parameters, significant memory consumption, and slow inference.

##### 4.3. Fully Convolutional Net

To address limitations in CNNs, Long et al. (2015) devised a fully convolutional network (FCN) by transforming fully connected layers in the default CNN with convolutional layers that enabled taking input of arbitrary size and generating correspondingly sized output. While the FCN can be efficiently applied to an image or volume, the use of convolution layers with filters larger than  $1 \times 1$  and max-pooling layers or strided convolutions lead to a reduction in data dimension resulting in a very low resolution in the output than in the input. In order to circumvent this limitation, the authors in (Long et al., 2015) applied the concept of up-sampling path using deconvolution operations to restore the spatial size of the down-sampled feature maps to the original input dimensions. Inspired by FCN architecture, Badrinarayanan et al. (2017) proposed an encoder-decoder network architecture for semantic pixel-wise segmentation called *SegNet*. Each max-pooling layer in the encoder part has a corresponding up-sampling layer in the decoder, which restores the

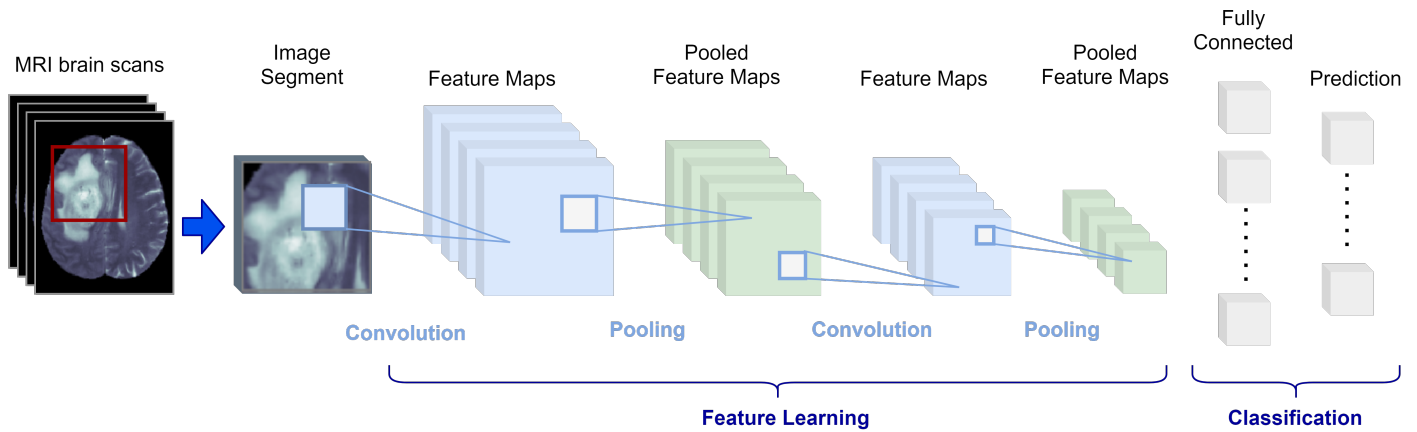


Figure 3: Patch-wise segmentation with CNN architecture. The input to the CNN is an image patch and the output is the probabilities for each class where the prediction for center pixel is the class with the highest score.

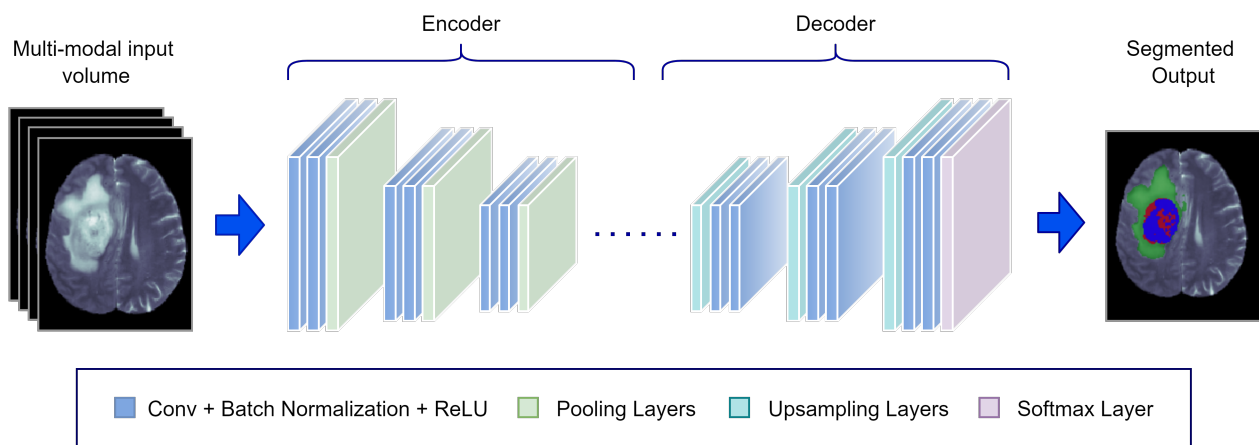


Figure 4: A schematic illustration of semantic-wise brain tumor segmentation with a SegNet-like architecture. The down-sampling through pooling layers in the encoder part of the network is compensated by the up-sampling layers in the decoder part that results in a segmentation output with dimensions same as the original input image.

feature maps to the original resolution. The softmax layer makes pixel-wise predictions and generates the final segmentation output which has dimensions same as the original input image. Recent successful segmentation networks are mostly based on convolutional encoder-decoder architectures. An illustration of semantic-wise brain tumor segmentation with a SegNet-like architecture is depicted in Fig. 4.

FCN and its variants have been extended to 3D for voxel classification, for instance, a 3D CNN consisting of two interconnected pathways, specifically, a convolutional and deconvolutional pathway, was proposed by Brosch et al. (2016) for multiple sclerosis lesion segmentation in MRI. They connected the first convolution layer and the last deconvolution layer through a single skip connection as a joint learning strategy of the feature extraction and prediction pathways and achieved superior performance when compared with five publicly available methods for this task. In the study by Dolz et al. (2018), a 3D FCN model capable of performing volume-to-volume learning to segment subcortical structure is proposed to combat the computational and memory requirements in regular 3D CNN. They investigated the effect of small kernels which enabled deeper architectures and achieved promising results.

#### 4.4. Biomedical Image Segmentation with U-Net

Ronneberger et al. (2015) proposed U-Net architecture comprised of a contracting path and an expanding path, which has become the dominant approach for segmentation in most recent applications. While it is similar to FCN, the architectural novelty in U-Net lies in the fact that the up-sampling and down-sampling layers are combined by skip connections to connect the opposing convolution and deconvolution layers. Later several variants of U-Net capable of performing 3D volume-to-volume segmentation were proposed with significant improvements. For instance, Çiçek et al. (2016) proposed a 3D U-Net by replacing 2D operations in 2D U-Net with their 3D equivalents and Milletari et al. (2016) implemented a 3D-variant of U-Net architecture using residual blocks, called V-net. These architectures are trained on entire images or large image patches as opposed to small patches and hence affected by data scarcity, which is typically addressed through data transformations such as shifting, rotating, scaling, or through applications of random deformations.

Efficient DNN-based medical image segmentation is often driven by the recent progress in semantic segmentation. In (Kayalibay et al., 2017), authors employed a network architecture similar to 3D U-Net for bone and brain tumor segmentation. They combined multiple segmentation maps created at differ-

ent scales which was shown to speed up convergence. However, this approach can be computationally expensive as they employed large receptive fields in convolutional layers. Isensee et al. (2017) implemented a 3D U-Net that has been modified with respect to up-sampling pathways, normalization methods, number of filters, and the batch size, enabling training with large image patches and capturing contextual information that leads to segmentation performance improvements. In a more recent work (Chen et al., 2018a), a separable 3D U-Net consisting of sparable 3D convolutions was proposed. Their S3D-UNet architecture fully utilizes the 3D volumes via the use of several 3D U-Net blocks. Isensee et al. (2018) argue that a well-designed U-Net architecture is competent in generating state-of-the-art segmentation maps without the need for significant architectural modifications and that enhancements proposed in prior literature provide no additional benefit. It should be highlighted that the winning contributions of Brain Tumor Segmentation (BRATS) challenge in 2019 (Jiang et al., 2019) and 2020 (Isensee et al., 2020) have also adopted U-Net-based architectures. Jiang et al. (2019) utilized a two-stage cascaded U-Net and Isensee et al. (2020) employed the nnU-Net architecture (Isensee et al., 2019) which was initially developed as a general-purpose network for segmentation following a U-Net.

#### 4.5. Deep Generative models

Supervised learning methods require large manually annotated data sets and do not generalize well for previously unseen pathological appearances. Alternatively, deep generative models facilitate unsupervised training and provide a mathematically grounded framework for learning hidden structures and complex distributions from unlabeled data. Here we briefly discuss two main subsets of deep generative models, variational autoencoders (AEs) (Kingma and Welling, 2013) and generative adversarial networks (GANs) (Goodfellow et al., 2014) and their applications in the realm of biomedical imaging (Salakhutdinov, 2015; Yi et al., 2019).

##### 4.5.1. Variational Auto-encoders

An autoencoder (AE) is composed of an inference network (encoder) that learns a mapping from the high-dimensional input  $\mathbf{x} \in \mathcal{X}$  to a lower-dimensional latent representation  $\mathbf{z} \in \mathcal{Z}$ , and a generator network (decoder) that reconstructs the data in latent space to a reconstruction  $\mathbf{x}'$ , where the input space is  $\mathcal{X} = \mathbb{R}^D$  and the latent space is  $\mathcal{Z} = \mathbb{R}^d$ . VAEs provide a probabilistic interpretation for variables in latent space by projecting input data onto a distribution. The prior distribution in the latent representation is typically a multivariate Gaussian, denoted by  $p_\theta(\mathbf{z}) = \mathcal{N}(0, \mathbb{I}_d)$ . The conditional distribution  $p_\theta(\mathbf{x}|\mathbf{z})$  parametrized by  $\theta$  represents the likelihood of generating a true data sample, given the sampled latent vector, which is usually defined as  $p_\theta(\mathbf{x}|\mathbf{z}) = \mathcal{N}(\mathbf{x}|\mu_\theta(\mathbf{z}), \mathbb{I}_D \sigma_\theta^2(\mathbf{z}))$ . The corresponding posterior distribution  $p_\theta(\mathbf{z}|\mathbf{x})$  is analytically intractable and hence it is approximated by a variational distribution  $q_\phi(\mathbf{z}|\mathbf{x})$ , parametrized by  $\phi$ . In practice, the probabilistic encoder parameterizes the latent distribution and maps input data onto a mean ( $\mu$ ) and variance ( $\sigma$ ) vector which are the parameters of the multivariate Gaussian. Latent distribution is then randomly sampled to feed into the probabilistic decoder that parameterizes

the likelihood distribution  $p_\theta(\mathbf{x}|\mathbf{z})$  and projects the latent space attributes back to the original domain space.

Owing to their ability to model the distribution that characterizes data, these models enable density-based anomaly detection and have received significant attention in clinical imaging. In MRI analysis, VAEs typically address detection of brain pathology via an unsupervised abnormality detection approach, where the distribution of healthy brain anatomy  $\mathbf{x} \in \mathcal{X}_{healthy}$  is modeled, which enables detection of pathologies as outliers of the distribution (Baur et al., 2021; Chen et al., 2018b). In (Chen and Konukoglu, 2018), authors investigated the performance of VAEs and adversarial auto-encoders on unsupervised lesion segmentation where they used a prior distribution of healthy brain tissues to detect any abnormalities. They further proposed a latent constraint to improve latent space consistency. Baur et al. (2018), presented a spatial VAE based deep generative model that captures the global context of MR slices instead of local patches. A schematic illustration of brain MRI reconstruction with VAE model based on multivariate Gaussian assumption is presented in Fig. 5.

##### 4.5.2. Generative adversarial networks

Initially introduced for image synthesis from noise, GANs made a huge impact on computer vision. Composed of a generator that generates new data by learning a latent representation of the training data from a prior distribution, and a discriminator that discriminates between real and synthetic data, the network is designed to compete against the two components during training, which is referred to as adversarial training. The same notion can be applied in segmentation by devising a segmentation network in place of the generator such that the discriminator distinguishes the input segmentation mask between the manually annotated ground truth and the segmentation map predicted by the network (Fig. 6). This forces the segmentation network to generate segmentation maps that are more anatomically plausible. In the seminal work by Luc et al. (2016), the authors applied an adversarial training approach for semantic segmentation, which is arguably the first study to utilize adversarial training to learn semantic segmentation models. They trained a convolutional net coupled with an adversarial network that can discriminate between a segmentation map from ground truth and model prediction, thus, facilitating the regularization of the segmentation and the results showed improved accuracy. In the case of tumor segmentation, Kamnitsas et al. (2017b) explored the performance of adversarial networks on domain adaptation and showed that their approach is robust to domain shift and does not require manual annotation of labels when applied to new data in the testing phase. This strategy of employing GANs for brain tumor segmentation was later followed by many other studies (Yu et al., 2018; Nema et al., 2020) incorporating several modifications. Notable is the *Segan* (Xue et al., 2018) introduced for medical image segmentation where they show that single scalar output of real or fake in classic GANs is ineffective and proposed an adversarial critic network with a multi-scale  $L_1$  loss function.

*summary:* Despite the demand for a large amount of data and the lack of model interpretability, medical image segmentation has seen a massive influx of methods associated with deep learning methods. Different strategies have been proposed in past literature to optimize the task of segmentation which has led to

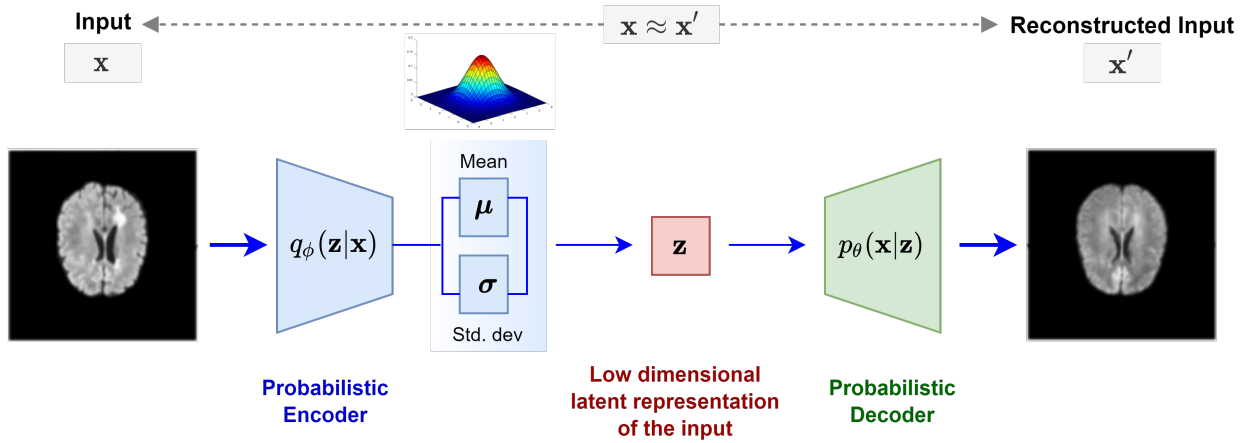


Figure 5: Reconstruction of a healthy brain MRI using a VAE model with Multivariate Gaussian assumption.

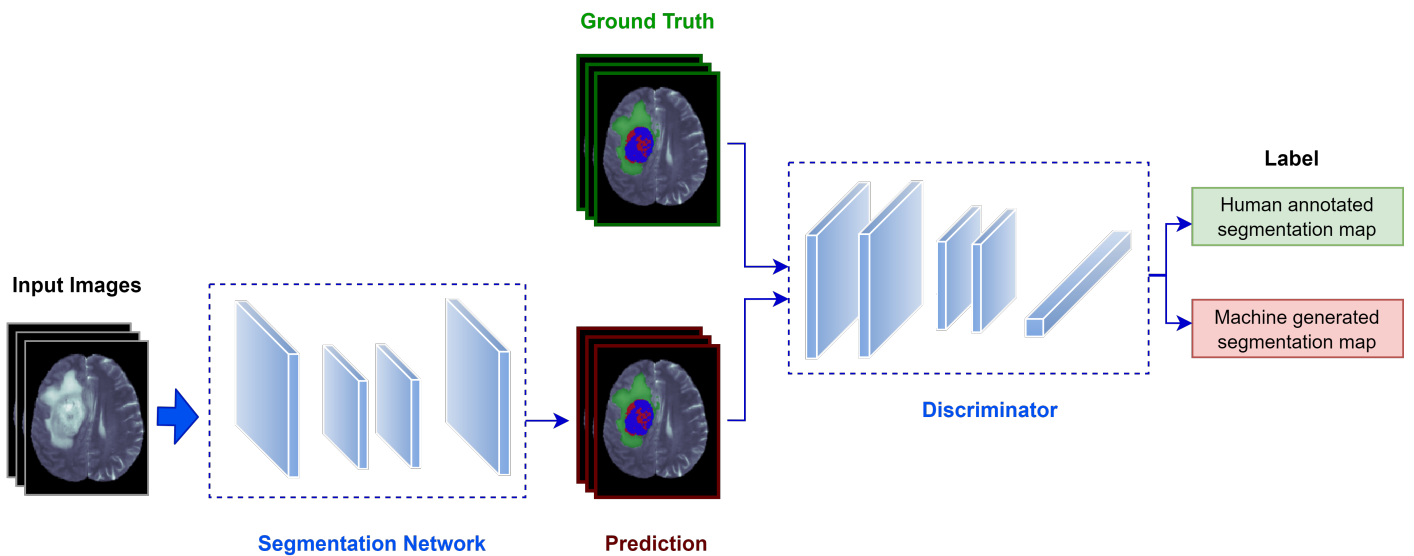


Figure 6: Adversarial training for tumor segmentation. Segmentation network generates segmentation maps and discriminator distinguishes between the manually annotated and predicted segmentation maps.

significant improvements in the development of fully automated diagnosis systems.

## 5. Integrated Statistical and Probabilistic Deep Learning methods for MRI Segmentation

There has been a recent surge of interest in approaches that leverage deep probabilistic models in segmentation. These methods are a step toward bridging the gap between traditional statistical methods of segmentation and modern deep learning-based segmentation, which enables the implementation of models that significantly benefit from both streams. Deep and statistical learning based integrated methods have great utility in a multitude of tasks, some of which are briefly discussed here.

*Data set Limitations/ Scarce Annotations:* Probabilistic deep learning has proved to be useful when training with limited data and sparse annotations. Dalca et al. (2019) combined probabilistic atlas-based segmentation with deep learning to develop an unsupervised brain MRI segmentation model. They showed

that their approach achieves promising results in terms of accuracy without the need for annotated data at test time and thus computationally efficient. Ito et al. (2019) modeled the tumor segmentation as a semi-supervised learning problem based on a CNN using a small number of labeled images and a large number of unlabeled images where they use image registration to attach a pseudo-label for every voxel. Since the true labels of the unlabeled images were unknown, they merged a probabilistic framework in their CNN model using the EM algorithm. While E-step performs a maximum a posteriori estimation for the hidden true label of unlabeled images, the M-step updates the parameters of the CNN model based on the estimated true labels. Their experimental results suggested that their approach achieves accurate and stable segmentation than the models trained relying only on DNN-based methods.

*Segmentation Refinement:* Voxel-based classification methodologies sometimes result in spurious responses and therefore, graphical-based models such as MRFs (Shakeri et al., 2016) and CRFs (Kamnitsas et al., 2017c; Lafferty et al., 2001; Chen et al., 2017; Dou et al., 2017; Zhao et al., 2018) are often integrated

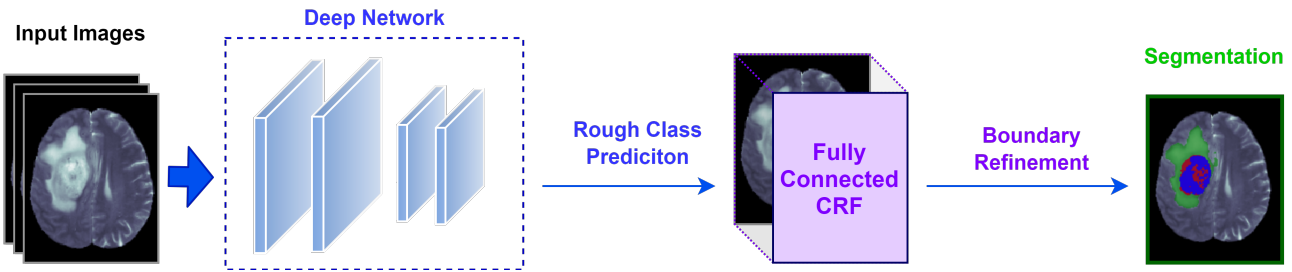


Figure 7: Schematic illustration of post segmentation refinement with a fully connected CRF that operates on the entire segmentation map generated by the deep network to refine coarse voxel-level predictions.

into likelihood maps generated by CNNs as post-processing to refine the segmentation which acts as label regularizers (Fig. 7). CRFs are probabilistic models that consider the contextual information, which allows to model voxels neighborhoods that are arbitrarily large. More specifically, CRFs model the conditional probability distribution of target pixel labels given the prediction distribution for each pixel. There are several different variants of post-segmentation refinement strategies with CRF such as fully-connected CRF (FC-CRF) that operates over the whole segmentation map, locally connected CRF that smoothens local patches, and CRFs formulated as recurrent neural networks (RNN-CRF) (Zheng et al., 2015) that allow end-to-end training with the segmentation network. In the realm of tumor segmentation, Kamnitsas et al. (2017c) used a 3D CNN model in conjunction with a 3D fully connected CRF for segmenting brain lesions from 3D medical scans. While the 3D CNN model generates soft segmentation maps, CRF acts as a post-processing step that produces final refined segmentation labels. Instead of applying CRFs as a post-processing step of FCNNs, Zhao et al. (2018) suggested integration of FCNNs and CRFs as one deep network. They used 2D image patches and image slices in axial, coronal, and sagittal views, and trained three models, which were then combined for segmentation of brain tumors and their results indicated that FCNN-CRF combination improves segmentation robustness.

**Uncertainty Quantification:** There are several other areas such as uncertainty estimation where the integration of traditional statistical learning methods with deep learning becomes beneficial. Quantifying deep network prediction uncertainty arising from data set limitations or intrinsic biological noise is often necessary. Prior studies have investigated uncertainty quantification with Bayesian neural networks (Kendall et al., 2015; Gal and Ghahramani, 2016) and their applicability to biomedical imaging in the context of brain segmentation (Jena and Awate, 2019; Roy et al., 2019; Kwon et al., 2020). In (Jena and Awate, 2019) authors show that uncertainty can be estimated analytically at test time through a Bayesian DL framework. Their experimental results on multiple biomedical imaging data sets indicated improved segmentation and calibration performance. Thus, prior research suggests that employing Bayesian deep nets for brain segmentation is a promising direction for obtaining uncertainty estimates and the robustness level required for clinically deployed automated systems.

**Generalizability:** Some recent studies (Agn et al., 2019; Cerri et al., 2021) have indicated that integrated methods can successfully be applied to improve generalizability. For example, Cerri et al. (2021) presented a method for simultaneous segmentation

of whole-brain and lesions by utilizing both a generative model and a deep net and demonstrated their approach is contrast adaptive.

In summary, it could be argued that the future path for medical decisions with computer-aided systems lies in the merging of statistical methodologies with deep learning-based methods.

## 6. Limitations, challenges and future directions in biomedical image analysis

### 6.1. Limitations and challenges

Medical image segmentation encompasses a broad set of challenges including complex and subtle surrounding boundaries of organs, lack of sufficient level of the region uniformity and similarity, low contrast and intensity inhomogeneity, image noise, partial volume effect, and other artifacts that impede precise identification of abrupt variations between organs of interest. Class imbalance, data acquisition, and 3D nature of data poses additional challenges, which are briefly described here.

**Class imbalance** presents one of the biggest difficulties in segmentation. For example, the tumor region typically constitutes only up to 15% of the brain, and tumor sub-regions are even smaller, and thus the class distribution is dominated by the background voxels when compared with the foreground voxels of tumor tissues. Prior work propose several strategies to address imbalanced distributions which include applying a weight map to the categorical cross-entropy loss function or incorporation of different loss functions such as focal loss (Lin et al., 2017). A recently introduced dynamically weighted balanced loss (Fernando and Tsokos, 2021) focuses on dynamically adjusting class weights to address the class imbalance which also leads to improved calibration. In the context of tumor segmentation, weighted dice loss is a commonly adopted approach (Milletari et al., 2016). Devising algorithms that are adept at dealing with class imbalance is imperative in medical image analysis.

Another primary limitation in biomedical imaging is the *acquisition of labeled data*. While computer-aided systems make the diagnosis process more efficient, supervised deep architectures require access to large, labeled data sets. Manual annotation requires domain expertise, and it is time-consuming. Since small data sets lack generalizability, deployment of semi or unsupervised architectures may be more effective.

**3D neuroimaging data** are memory intensive. In order to utilize contextual information in brain volumetry on MR images, 3D deep networks are typically deployed, which uses extensive

memory. Previous research adopts different techniques to address this issue which include training on 2D slices or image patches and employing multi-path models. However, regulating the trade-off between leveraging the spatial context of neighboring voxels and computational complexity continues to be a challenge.

## 6.2. Future Directions

The transition from scientific research to clinical practice depends on the trustworthiness of computer-aided diagnosis systems and raises profound questions about reliability, uncertainty, and robustness. For example, how to detect when the computational algorithms get it wrong? Can we predict when the machine learning model fails, and how to make the algorithm robust to changes in real-world conditions and clinical data? These research questions are of central interest in safety-critical medical applications where accuracy is integral. Here we briefly discuss some of the critical challenges and potential future directions in medical image analysis.

- Learning the right features: The performance of the diagnosis system should not be influenced by the variability across different scanners, settings of the image acquisition, or other clinical conditions of patients. Learning discriminative features which are generalizable representations across data sets is an active area of research, however, until substantial progress is made in robustness research, care should be taken when relying on these strategies where precision is vital.
- Knowing when the model does not know: Quantifying uncertainty in tumor segmentation is indispensable in clinical decision making (Begoli et al., 2019; Jungo and Reyes, 2019). While deep learning-based approaches have achieved remarkable success performance-wise, their practical applicability is limited as models do not produce a measure for prediction uncertainty. We expect the research on uncertainty estimation in neuroimaging to increase in the near future.
- Detecting when an automated system fails: Deep network based methods are prone to overfitting and hence evaluating the level of accuracy on new clinical data in the absence of ground truth is crucial in automated diagnosis. Methods are required to identify when the system fails and to evaluate the actual performance after implementation when a reference segmentation by an expert is inaccessible. This has been previously evaluated only to a very limited extent (Valindria et al., 2017). Future efforts should further explore this issue before clinical adoption of automated systems.
- Going beyond human-level performance: The ultimate goal in computer-aided medical screening is to surpass human-level performance. Cancer histopathology reads in biomedical imaging requires expert knowledge, and it may be subject to annotation bias while leading to a lack of agreement among human experts and therefore identifying the exact ground truth segmentation could be challenging. Synthesis of ground truth via adversarial learning appears to be a promising research direction in this context.

## 7. Conclusion

Precise tumor delineation is imperative for accurate assessment of the relative volume of lesion sub-components. A comprehensive review is conducted on the state-of-the-art brain tumor segmentation of 3D MRI ranging from traditional statistical approaches to modern deep learning. We covered the fundamentals, discussed the methodological foundations, and addressed their potentials and limitations. The review conducted leads to the following conclusions: deep learning, being capable of learning high-level feature representations automatically, has emerged as a powerful mechanism in automated volumetric medical image segmentation. Moreover, it has been observed that engrafting statistical methodologies in deep networks improve biomedical image segmentation. Thus, volumetric 3D MRI segmentation at the intersection of statistical modeling and deep learning can be considered as a more effective alternative to the methods which are purely statistical or deep learning based. While these automated methodologies improve the qualitative expertise of clinicians and facilitate accurate volumetric tumor delineation and outcome prediction, they mostly remain in the pre-clinical research domain. Although studies have been conducted by many researchers for 3D volumetric tumor segmentation, difficulties associated with biomedical imaging are still insufficiently studied and the deployment of robust automated systems is a challenge for future research to explore. Future studies could fruitfully investigate these issues further by more systematic and theoretical analysis.

## References

- Aerts, H.J., Velazquez, E.R., Leijenaar, R.T., Parmar, C., Grossmann, P., Carvalho, S., Bussink, J., Monshouwer, R., Haihe-Kains, B., Riethoven, D., et al., 2014. Decoding tumour phenotype by noninvasive imaging using a quantitative radiomics approach. *Nature communications* 5, 1–9.
- Agn, M., af Rosenschöld, P.M., Puonti, O., Lundemann, M.J., Mancini, L., Papadaki, A., Thust, S., Ashburner, J., Law, I., Van Leemput, K., 2019. A modality-adaptive method for segmenting brain tumors and organs-at-risk in radiation therapy planning. *Medical image analysis* 54, 220–237.
- Arnold, J.B., Liow, J.S., Schaper, K.A., Stern, J.J., Sled, J.G., Shattuck, D.W., Worth, A.J., Cohen, M.S., Leahy, R.M., Mazziotta, J.C., et al., 2001. Qualitative and quantitative evaluation of six algorithms for correcting intensity nonuniformity effects. *NeuroImage* 13, 931–943.
- Badrinarayanan, V., Kendall, A., Cipolla, R., 2017. Segnet: A deep convolutional encoder-decoder architecture for image segmentation. *IEEE transactions on pattern analysis and machine intelligence* 39, 2481–2495.
- Banik, S., Rangayyan, R.M., Boag, G.S., 2009. Landmarking and segmentation of 3d ct images. *Synthesis lectures on biomedical engineering* 4, 1–170.
- Bauer, S., Nolte, L.P., Reyes, M., 2011. Segmentation of brain tumor images based on atlas-registration combined with a markov-random-field lesion growth model, in: 2011 IEEE International Symposium on Biomedical Imaging: From Nano to Macro, IEEE. pp. 2018–2021.
- Baur, C., Denner, S., Wiestler, B., Navab, N., Albarqouni, S., 2021. Autoencoders for unsupervised anomaly segmentation in brain mr images: A comparative study. *Medical Image Analysis* , 101952.
- Baur, C., Wiestler, B., Albarqouni, S., Navab, N., 2018. Deep autoencoding models for unsupervised anomaly segmentation in brain mr images, in: International MICCAI Brainlesion Workshop, Springer. pp. 161–169.

- Begoli, E., Bhattacharya, T., Kusnezov, D., 2019. The need for uncertainty quantification in machine-assisted medical decision making. *Nature Machine Intelligence* 1, 20–23.
- Belaroussi, B., Milles, J., Carme, S., Zhu, Y.M., Benoit-Cattin, H., 2006. Intensity non-uniformity correction in mri: existing methods and their validation. *Medical image analysis* 10, 234–246.
- Bi, W.L., Hosny, A., Schabath, M.B., Giger, M.L., Birkbak, N.J., Mehrtash, A., Allison, T., Arnaout, O., Abbosh, C., Dunn, I.F., et al., 2019. Artificial intelligence in cancer imaging: clinical challenges and applications. *CA: a cancer journal for clinicians* 69, 127–157.
- Brosch, T., Tang, L.Y., Yoo, Y., Li, D.K., Traboulsee, A., Tam, R., 2016. Deep 3d convolutional encoder networks with shortcuts for multi-scale feature integration applied to multiple sclerosis lesion segmentation. *IEEE transactions on medical imaging* 35, 1229–1239.
- Capelle, A.S., Alata, O., Fernandez, C., Lefèvre, S., Ferrie, J., 2000. Unsupervised segmentation for automatic detection of brain tumors in mri, in: *Proceedings 2000 International Conference on Image Processing (Cat. No. 00CH37101)*, IEEE. pp. 613–616.
- Cerri, S., Puonti, O., Meier, D.S., Wuerfel, J., Mühlau, M., Siebner, H.R., Van Leemput, K., 2021. A contrast-adaptive method for simultaneous whole-brain and lesion segmentation in multiple sclerosis. *NeuroImage* 225, 117471.
- Chen, L.C., Papandreou, G., Kokkinos, I., Murphy, K., Yuille, A.L., 2017. Deeplab: Semantic image segmentation with deep convolutional nets, atrous convolution, and fully connected crfs. *IEEE transactions on pattern analysis and machine intelligence* 40, 834–848.
- Chen, W., Liu, B., Peng, S., Sun, J., Qiao, X., 2018a. S3d-unet: separable 3d u-net for brain tumor segmentation, in: *International MICCAI Brainlesion Workshop*, Springer. pp. 358–368.
- Chen, X., Konukoglu, E., 2018. Unsupervised detection of lesions in brain mri using constrained adversarial auto-encoders. *arXiv preprint arXiv:1806.04972*.
- Chen, X., Pawlowski, N., Rajchl, M., Glocker, B., Konukoglu, E., 2018b. Deep generative models in the real-world: An open challenge from medical imaging. *arXiv preprint arXiv:1806.05452*.
- Çiçek, Ö., Abdulkadir, A., Lienkamp, S.S., Brox, T., Ronneberger, O., 2016. 3d u-net: learning dense volumetric segmentation from sparse annotation, in: *International conference on medical image computing and computer-assisted intervention*, Springer. pp. 424–432.
- Ciresan, D., Giusti, A., Gambardella, L., Schmidhuber, J., 2012. Deep neural networks segment neuronal membranes in electron microscopy images. *Advances in neural information processing systems* 25, 2843–2851.
- Cordova, J.S., Schreiber, E., Hadjipanayis, C.G., Guo, Y., Shu, H.K.G., Shim, H., Holder, C.A., 2014. Quantitative tumor segmentation for evaluation of extent of glioblastoma resection to facilitate multisite clinical trials. *Translational oncology* 7, 40–W5.
- Corso, J.J., Sharon, E., Dube, S., El-Saden, S., Sinha, U., Yuille, A., 2008. Efficient multilevel brain tumor segmentation with integrated bayesian model classification. *IEEE transactions on medical imaging* 27, 629–640.
- Dalca, A.V., Yu, E., Golland, P., Fischl, B., Sabuncu, M.R., Iglesias, J.E., 2019. Unsupervised deep learning for bayesian brain mri segmentation, in: *International Conference on Medical Image Computing and Computer-Assisted Intervention*, Springer. pp. 356–365.
- DeCarli, C., Maisog, J., Murphy, D.G., Teichberg, D., Rapoport, S.I., Horwitz, B., 1992. Method for quantification of brain, ventricular, and subarachnoid csf volumes from mr images. *Journal of computer assisted tomography* 16, 274–284.
- Despotović, I., Goossens, B., Philips, W., 2015. Mri segmentation of the human brain: challenges, methods, and applications. *Computational and mathematical methods in medicine*.
- Dolz, J., Desrosiers, C., Ayed, I.B., 2018. 3d fully convolutional networks for subcortical segmentation in mri: A large-scale study. *NeuroImage* 170, 456–470.
- Dou, Q., Yu, L., Chen, H., Jin, Y., Yang, X., Qin, J., Heng, P.A., 2017. 3d deeply supervised network for automated segmentation of volumetric medical images. *Medical image analysis* 41, 40–54.
- Doyle, S., Vasseur, F., Dojat, M., Forbes, F., 2013. Fully automatic brain tumor segmentation from multiple mr sequences using hidden markov fields and variational em. *Procs. NCI-MICCAI BraTS*, 18–22.
- Farabet, C., Couprie, C., Najman, L., LeCun, Y., 2012. Learning hierarchical features for scene labeling. *IEEE transactions on pattern analysis and machine intelligence* 35, 1915–1929.
- Fernando, K.R.M., Tsokos, C.P., 2021. Dynamically weighted balanced loss: Class imbalanced learning and confidence calibration of deep neural networks. *IEEE Transactions on Neural Networks and Learning Systems*, 1–12doi:10.1109/TNNLS.2020.3047335.
- Gal, Y., Ghahramani, Z., 2016. Dropout as a bayesian approximation: Representing model uncertainty in deep learning, in: *international conference on machine learning*, PMLR. pp. 1050–1059.
- Gering, D.T., Grimson, W.E.L., Kikinis, R., 2002. Recognizing deviations from normalcy for brain tumor segmentation, in: *International Conference on Medical Image Computing and Computer-Assisted Intervention*, Springer. pp. 388–395.
- Gonzalez, R.C., Woods, R.E., 2006. *Digital Image Processing (3rd Edition)*. Prentice-Hall, Inc., USA.
- Goodfellow, I., Pouget-Abadie, J., Mirza, M., Xu, B., Warde-Farley, D., Ozair, S., Courville, A., Bengio, Y., 2014. Generative adversarial nets. *Advances in neural information processing systems* 27, 2672–2680.
- Grimson, W.E.L., Ettinger, G., Kapur, T., Leventon, M.E., Wells III, W.M., Kikinis, R., 1997. Utilizing segmented mri data in image-guided surgery. *International Journal of Pattern Recognition and Artificial Intelligence* 11, 1367–1397.
- Havaei, M., Davy, A., Warde-Farley, D., Biard, A., Courville, A., Bengio, Y., Pal, C., Jodoin, P.M., Larochelle, H., 2017. Brain tumor segmentation with deep neural networks. *Medical image analysis* 35, 18–31.
- Hong, T.S., Tomé, W.A., Harari, P.M., 2012. Heterogeneity in head and neck imrt target design and clinical practice. *Radiotherapy and Oncology* 103, 92–98.
- Isensee, F., Jaeger, P.F., Full, P.M., Vollmuth, P., Maier-Hein, K.H., 2020. nnu-net for brain tumor segmentation. *arXiv preprint arXiv:2011.00848*.
- Isensee, F., Jäger, P.F., Kohl, S.A., Petersen, J., Maier-Hein, K.H., 2019. Automated design of deep learning methods for biomedical image segmentation. *arXiv preprint arXiv:1904.08128*.
- Isensee, F., Kickingereder, P., Wick, W., Bendszus, M., Maier-Hein, K.H., 2017. Brain tumor segmentation and radiomics survival prediction: Contribution to the brats 2017 challenge, in: *International MICCAI Brainlesion Workshop*, Springer. pp. 287–297.
- Isensee, F., Kickingereder, P., Wick, W., Bendszus, M., Maier-Hein, K.H., 2018. No new-net, in: *International MICCAI Brainlesion Workshop*, Springer. pp. 234–244.
- Ito, R., Nakae, K., Hata, J., Okano, H., Ishii, S., 2019. Semi-supervised deep learning of brain tissue segmentation. *Neural Networks* 116, 25–34.
- Jena, R., Awate, S.P., 2019. A bayesian neural net to segment images with uncertainty estimates and good calibration, in: *International Conference on Information Processing in Medical Imaging*, Springer. pp. 3–15.
- Jiang, Z., Ding, C., Liu, M., Tao, D., 2019. Two-stage cascaded u-net: 1st place solution to brats challenge 2019 segmentation task, in: *International MICCAI Brainlesion Workshop*, Springer. pp. 231–241.
- Jungo, A., Reyes, M., 2019. Assessing reliability and challenges of uncertainty estimations for medical image segmentation, in: *International Conference on Medical Image Computing and Computer-Assisted Intervention*, Springer. pp. 48–56.
- Kalavathi, P., Prasath, V.S., 2016. Methods on skull stripping of mri head scan images—a review. *Journal of digital imaging* 29, 365–379.
- Kamnitsas, K., Bai, W., Ferrante, E., McDonagh, S., Sinclair, M., Pawlowski, N., Rajchl, M., Lee, M., Kainz, B., Rueckert, D., et al., 2017a. Ensembles of multiple models and architectures for robust

- brain tumour segmentation, in: International MICCAI brainlesion workshop, Springer. pp. 450–462.
- Kamnitsas, K., Baumgartner, C., Ledig, C., Newcombe, V., Simpson, J., Kane, A., Menon, D., Nori, A., Criminisi, A., Rueckert, D., et al., 2017b. Unsupervised domain adaptation in brain lesion segmentation with adversarial networks, in: International conference on information processing in medical imaging, Springer. pp. 597–609.
- Kamnitsas, K., Ledig, C., Newcombe, V.F., Simpson, J.P., Kane, A.D., Menon, D.K., Rueckert, D., Glocker, B., 2017c. Efficient multi-scale 3d cnn with fully connected crf for accurate brain lesion segmentation. *Medical image analysis* 36, 61–78.
- Kayalibay, B., Jensen, G., van der Smagt, P., 2017. Cnn-based segmentation of medical imaging data. *arXiv preprint arXiv:1701.03056*.
- Kendall, A., Badrinarayanan, V., Cipolla, R., 2015. Bayesian segnet: Model uncertainty in deep convolutional encoder-decoder architectures for scene understanding. *arXiv preprint arXiv:1511.02680*.
- Kikinis, R., Gleason, P.L., Moriarty, T.M., Moore, M.R., Alexander, E., Stieg, P.E., Matsumae, M., Lorensen, W.E., Cline, H.E., Black, P.M., et al., 1996. Computer-assisted interactive three-dimensional planning neurosurgical procedures. *Neurosurgery* 38, 640–651.
- Kingma, D.P., Welling, M., 2013. Auto-encoding variational bayes. *arXiv preprint arXiv:1312.6114*.
- Koshy, M., Villano, J.L., Dolecek, T.A., Howard, A., Mahmood, U., Chmura, S.J., Weichselbaum, R.R., McCarthy, B.J., 2012. Improved survival time trends for glioblastoma using the seer 17 population-based registries. *Journal of neuro-oncology* 107, 207–212.
- Kosugi, Y., Watanabe, E., Goto, J., Watanabe, T., Yoshimoto, S., Takakura, K., Ikebe, J., 1988. An articulated neurosurgical navigation system using mri and ct images. *IEEE Transactions on Biomedical Engineering* 35, 147–152.
- Krizhevsky, A., Sutskever, I., Hinton, G.E., 2017. Imagenet classification with deep convolutional neural networks. *Communications of the ACM* 60, 84–90.
- Kwon, Y., Won, J.H., Kim, B.J., Paik, M.C., 2020. Uncertainty quantification using bayesian neural networks in classification: Application to biomedical image segmentation. *Computational Statistics & Data Analysis* 142, 106816.
- Lafferty, J., McCallum, A., Pereira, F.C., 2001. Conditional random fields: Probabilistic models for segmenting and labeling sequence data.
- Landini, L., Positano, V., Santarelli, M., 2018. Advanced image processing in magnetic resonance imaging. CRC press.
- LeCun, Y., Bengio, Y., Hinton, G., 2015. Deep learning. *nature* 521, 436–444.
- LeCun, Y., Haffner, P., Bottou, L., Bengio, Y., 1999. Object recognition with gradient-based learning, in: Shape, contour and grouping in computer vision. Springer, pp. 319–345.
- Li, S.Z., 2009. Mathematical mrf models, in: Markov random field modeling in image analysis. Springer, pp. 1–28.
- Lin, T.Y., Goyal, P., Girshick, R., He, K., Dollár, P., 2017. Focal loss for dense object detection, in: Proceedings of the IEEE international conference on computer vision, pp. 2980–2988.
- Lipková, J., Angelikopoulos, P., Wu, S., Alberts, E., Wiestler, B., Diehl, C., Preibisch, C., Pyka, T., Combs, S.E., Hadjidakis, P., et al., 2019. Personalized radiotherapy design for glioblastoma: integrating mathematical tumor models, multimodal scans, and bayesian inference. *IEEE transactions on medical imaging* 38, 1875–1884.
- Long, J., Shelhamer, E., Darrell, T., 2015. Fully convolutional networks for semantic segmentation, in: Proceedings of the IEEE conference on computer vision and pattern recognition, pp. 3431–3440.
- Luc, P., Couprie, C., Chintala, S., Verbeek, J., 2016. Semantic segmentation using adversarial networks. *arXiv preprint arXiv:1611.08408*.
- Mackay, A., Burford, A., Carvalho, D., Izquierdo, E., Fazal-Salom, J., Taylor, K.R., Bjerke, L., Clarke, M., Vinci, M., Nandhabalan, M., et al., 2017. Integrated molecular meta-analysis of 1,000 pediatric high-grade and diffuse intrinsic pontine glioma. *Cancer cell* 32, 520–537.
- Menze, B.H., Jakab, A., Bauer, S., Kalpathy-Cramer, J., Farahani, K., Kirby, J., Burren, Y., Porz, N., Slotboom, J., Wiest, R., et al., 2014. The multimodal brain tumor image segmentation benchmark (brats). *IEEE transactions on medical imaging* 34, 1993–2024.
- Menze, B.H., Van Leemput, K., Lashkari, D., Riklin-Raviv, T., Geremia, E., Alberts, E., Gruber, P., Wegener, S., Weber, M.A., Székely, G., et al., 2015. A generative probabilistic model and discriminative extensions for brain lesion segmentation—with application to tumor and stroke. *IEEE transactions on medical imaging* 35, 933–946.
- Milletari, F., Navab, N., Ahmadi, S.A., 2016. V-net: Fully convolutional neural networks for volumetric medical image segmentation, in: 2016 fourth international conference on 3D vision (3DV), IEEE. pp. 565–571.
- Moeskops, P., Viergever, M.A., Mendrik, A.M., De Vries, L.S., Benders, M.J., Išgum, I., 2016. Automatic segmentation of mr brain images with a convolutional neural network. *IEEE transactions on medical imaging* 35, 1252–1261.
- Moon, N., Bullitt, E., Van Leemput, K., Gerig, G., 2002. Model-based brain and tumor segmentation, in: Object recognition supported by user interaction for service robots, IEEE. pp. 528–531.
- Nema, S., Dudhane, A., Murala, S., Naidu, S., 2020. Rescuenet: An unpaired gan for brain tumor segmentation. *Biomedical Signal Processing and Control* 55, 101641.
- Nie, J., Xue, Z., Liu, T., Young, G.S., Setayesh, K., Guo, L., Wong, S.T., 2009. Automated brain tumor segmentation using spatial accuracy-weighted hidden markov random field. *Computerized Medical Imaging and Graphics* 33, 431–441.
- Patenaude, B., Smith, S.M., Kennedy, D.N., Jenkinson, M., 2011. A bayesian model of shape and appearance for subcortical brain segmentation. *Neuroimage* 56, 907–922.
- Pereira, S., Pinto, A., Alves, V., Silva, C.A., 2016. Brain tumor segmentation using convolutional neural networks in mri images. *IEEE transactions on medical imaging* 35, 1240–1251.
- Quail, D.F., Joyce, J.A., 2017. The microenvironmental landscape of brain tumors. *Cancer cell* 31, 326–341.
- Rajinikanth, V., Raja, N.S.M., Kamalanand, K., 2017. Firefly algorithm assisted segmentation of tumor from brain mri using tsallis function and markov random field. *Journal of Control Engineering and Applied Informatics* 19, 97–106.
- Ronneberger, O., Fischer, P., Brox, T., 2015. U-net: Convolutional networks for biomedical image segmentation, in: International Conference on Medical image computing and computer-assisted intervention, Springer. pp. 234–241.
- Roth, H.R., Lu, L., Liu, J., Yao, J., Seff, A., Cherry, K., Kim, L., Summers, R.M., 2015. Improving computer-aided detection using convolutional neural networks and random view aggregation. *IEEE transactions on medical imaging* 35, 1170–1181.
- Roth, H.R., Lu, L., Seff, A., Cherry, K.M., Hoffman, J., Wang, S., Liu, J., Turkbey, E., Summers, R.M., 2014. A new 2.5 d representation for lymph node detection using random sets of deep convolutional neural network observations, in: International conference on medical image computing and computer-assisted intervention, Springer. pp. 520–527.
- Roy, A.G., Conjeti, S., Navab, N., Wachinger, C., Initiative, A.D.N., et al., 2019. Bayesian quicknat: model uncertainty in deep whole-brain segmentation for structure-wise quality control. *NeuroImage* 195, 11–22.
- Salakhutdinov, R., 2015. Learning deep generative models. *Annual Review of Statistics and Its Application* 2, 361–385.
- Schad, L.R., Boesecke, R., Schlegel, W., Hartmann, G.H., Sturm, V., Strauss, L.G., Lorenz, W.J., 1987. Three dimensional image correlation of ct, mr, and pet studies in radiotherapy treatment planning of brain tumors. *Journal of computer assisted tomography* 11, 948–954.
- Setio, A.A.A., Ciompi, F., Litjens, G., Gerke, P., Jacobs, C., Van Riel, S.J., Wille, M.M.W., Naqibullah, M., Sánchez, C.I., van Ginneken, B., 2016. Pulmonary nodule detection in ct images: false positive reduction using multi-view convolutional networks. *IEEE transactions on medical imaging* 35, 1160–1169.

- Shakeri, M., Tsogkas, S., Ferrante, E., Lippe, S., Kadoury, S., Paragios, N., Kokkinos, I., 2016. Sub-cortical brain structure segmentation using f-cnn's, in: 2016 IEEE 13th International Symposium on Biomedical Imaging (ISBI), IEEE. pp. 269–272.
- Shattuck, D.W., Leahy, R.M., 2002. Brainsuite: an automated cortical surface identification tool. *Medical image analysis* 6, 129–142.
- Simonyan, K., Zisserman, A., 2014. Very deep convolutional networks for large-scale image recognition. *arXiv preprint arXiv:1409.1556*.
- Smith, S.M., 2002. Fast robust automated brain extraction. *Human brain mapping* 17, 143–155.
- Song, S., Zheng, Y., He, Y., 2017. A review of methods for bias correction in medical images. *Biomedical Engineering Review* 1.
- Suri, J.S., Setarehdan, S.K., Singh, S., 2001. *Advanced algorithmic approaches to medical image segmentation: state-of-the-art application in cardiology, neurology, mammography and pathology*. Springer-Verlag.
- Szegedy, C., Liu, W., Jia, Y., Sermanet, P., Reed, S., Anguelov, D., Erhan, D., Vanhoucke, V., Rabinovich, A., 2015. Going deeper with convolutions, in: *Proceedings of the IEEE conference on computer vision and pattern recognition*, pp. 1–9.
- Tustison, N.J., Avants, B.B., Cook, P.A., Zheng, Y., Egan, A., Yushkevich, P.A., Gee, J.C., 2010. N4itk: improved n3 bias correction. *IEEE transactions on medical imaging* 29, 1310–1320.
- Uwano, I., Kudo, K., Yamashita, F., Goodwin, J., Higuchi, S., Ito, K., Harada, T., Ogawa, A., Sasaki, M., 2014. Intensity inhomogeneity correction for magnetic resonance imaging of human brain at 7t. *Medical physics* 41, 022302.
- Valindria, V.V., Lavdas, I., Bai, W., Kamnitsas, K., Aboagye, E.O., Rockall, A.G., Rueckert, D., Glocker, B., 2017. Reverse classification accuracy: predicting segmentation performance in the absence of ground truth. *IEEE transactions on medical imaging* 36, 1597–1606.
- Van Leemput, K., Puonti, O., 2015. Tissue classification, in: *Brain Mapping: An Encyclopedic Reference: Volume 1: Acquisition Methods, Methods and Modeling*. Elsevier, pp. 373–381.
- Warfield, S.K., Zou, K.H., Wells, W.M., 2008. Validation of image segmentation by estimating rater bias and variance. *Philosophical Transactions of the Royal Society A: Mathematical, Physical and Engineering Sciences* 366, 2361–2375.
- Wright, I., McGuire, P., Poline, J.B., Travere, J., Murray, R., Frith, C., Frackowiak, R., Friston, K., 1995. A voxel-based method for the statistical analysis of gray and white matter density applied to schizophrenia. *Neuroimage* 2, 244–252.
- Xia, Y., Ji, Z., Zhang, Y., 2016. Brain mri image segmentation based on learning local variational gaussian mixture models. *Neurocomputing* 204, 189–197.
- Xue, Y., Xu, T., Zhang, H., Long, L.R., Huang, X., 2018. Segan: Adversarial network with multi-scale l1 loss for medical image segmentation. *Neuroinformatics* 16, 383–392.
- Yi, X., Walia, E., Babyn, P., 2019. Generative adversarial network in medical imaging: A review. *Medical image analysis* 58, 101552.
- Yu, B., Zhou, L., Wang, L., Fripp, J., Bourgeat, P., 2018. 3d cgan based cross-modality mr image synthesis for brain tumor segmentation, in: 2018 IEEE 15th International Symposium on Biomedical Imaging (ISBI 2018), IEEE. pp. 626–630.
- Zeng, X., Staib, L.H., Schultz, R.T., Duncan, J.S., 1998. Segmentation and measurement of the cortex from 3d mr images, in: *International Conference on Medical Image Computing and Computer-Assisted Intervention*, Springer. pp. 519–530.
- Zhang, Y., Brady, M., Smith, S., 2001. Segmentation of brain mr images through a hidden markov random field model and the expectation-maximization algorithm. *IEEE transactions on medical imaging* 20, 45–57.
- Zhao, X., Wu, Y., Song, G., Li, Z., Zhang, Y., Fan, Y., 2018. A deep learning model integrating fcnn and crfs for brain tumor segmentation. *Medical image analysis* 43, 98–111.
- Zheng, S., Jayasumana, S., Romera-Paredes, B., Vineet, V., Su, Z., Du, D., Huang, C., Torr, P.H., 2015. Conditional random fields as recurrent neural networks, in: *Proceedings of the IEEE international conference on computer vision*, pp. 1529–1537.
- Zikic, D., Ioannou, Y., Brown, M., Criminisi, A., 2014. Segmentation of brain tumor tissues with convolutional neural networks. *Proceedings MICCAI-BRATS*, 36–39.
- Zitova, B., Flusser, J., 2003. Image registration methods: a survey. *Image and vision computing* 21, 977–1000.